Jpn. J. Appl. Phys. Vol. 40 (2001) pp. 5837–5840
Part 1, No. 10, October 2001

Modelling of Structural and Threshold Voltage Characteristics of Randomly Doped Silicon Nanowires in the Coulomb-Blockade Regime

Gareth J. EVANS[1], Hiroshi MIZUTA[2,3] and Haroon AHMED[1,3]

[1]*Microelectronics Research Centre, Cavendish Laboratory, Madingley Road, Cambridge CB3 OHE, UK*
[2]*Hitachi Cambridge Laboratory, Cavendish Laboratory, Madingley Road, Cambridge CB3 OHE, UK*
[3]*CREST, Japan Science and Technology (JST)*

(Received May 8, 2001; accepted for publication July 4, 2001)

We report on the theoretical investigation of how geometrically uniform highly doped silicon nanowires can break up into a series of islands that exhibit Coulomb blockade. By using a newly developed numerical simulation in which random ionized dopants are introduced explicitly and the electron distribution is calculated self-consistently under the Thomas-Fermi approximation, we demonstrate natural formation of electron islands in the nanowires owing to the random dopant potential. We study the quasi-one-dimensional nature of the electron islands formed in the nanowires. The offset charge effects on the current threshold of the nanowire transistors are then investigated by feeding the derived structural parameters such as inter-island capacitance and tunnel resistance into a Monte Carlo single electron transport simulator. We show that the overall threshold voltage distribution can roughly be described as a two-'macro'-island system despite a complex series of multiple electron islands.

KEYWORDS: random ionized dopant, silicon nanowire, Coulomb blockade, single-electron tunneling, Thomas-Fermi approximation, Monte Carlo simulation

1. Introduction

For realising single- or few-electron memory and logic devices, the double or multiple tunnel junction (MTJ) structures are a key building block which exhibits the Coulomb blockade (CB) effect[1–3] and controls the transfer of a small number of electrons. From the device engineering point of view the MTJ structure is more suitable than the simple double tunnel junction since it reduces co-tunnelling which generally leads to unfavourable leakage current. Also the MTJ structure is robust against the offset charge effects[4–6] which vary the Coulomb gap and even may break the Coulomb blockade. The MTJ structures have been realised by using gated heavily doped silicon or GaAs nanowires with a few tens of nanometers in width. Although the nanowires are formed to be geometrically uniform, the electron distribution in the nanowires is not uniform because of randomly distributed dopant atoms and fluctuations in surface potentials, and isolated electron islands are naturally formed when the overall electron concentration becomes low under a negative gate bias. The nanowires can be formed either vertically[7] or laterally,[8] but the lateral structures have been used more often because of the simplicity of device fabrication. For the lateral nanowires the CB oscillation has been observed experimentally at a temperature up to around 60 K, and it has successfully been applied for making nanoscale memory[9–11] and logic devices.[12]

Despite the frequent use of the MTJs for device applications, the basic mechanism of the electron-island formation and electron transport properties in the heavily-doped nanowires have not yet been made clear. In this paper we explore two problems by using a newly developed simulation in which the randomly distributed ionised dopants in the nanowire are treated explicitly. The first is the way in which geometrically uniform wires break up into islands; although many mechanisms can be proposed, we consider solely the confining effect of the random dopant distribution. The second problem is the effect of uncontrolled offset charges which can gate the islands, so changing the electrical characteristics of the nanowire. Offset charge independence is a very important topic in all single-electron systems and its understanding and control are essential to building large scale digital logic. We model the electron distribution in random dopant potentials by extending an approach that Nixon and Davies[13] used to study low electron density quantum wires. We present results on structural parameters of the resulting electron distribution and of the electrical characteristics such structures would produce in the presence of random offset charges. This work may provide a theoretical framework in which to discuss and evaluate the potential of single electron devices.

2. Model and Numerical Simulation Method

In this work we use a simple model system, shown in the inset in Fig. 1. A silicon nanowire is assumed to be a 400-nm-long rectangular parallelepiped with a cross sectional area of 20 nm × 10 nm, and ionised dopant atoms are randomly placed over the entire volume of the nanowire. Such a geometrically and electrically simple system ensures that break-up into islands results only from random dopant placement. In addition, this system is computationally accessible whereas a full simulation of an actual experimental device would require

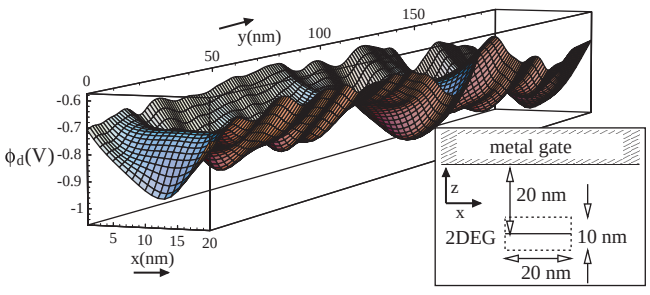

Fig. 1. Bare dopant potential ϕ_d landscape for a mean dopant concentration of 10^{25} m^{-3} and (inset) the simplified structure of our model. Electrons are confined to a two-dimensional area (perpendicular to the page.) Dopants positions are placed randomly (uniform distribution) in the dotted box.

undue computer time. Regarding the Coulomb-like potential around an individual ionised dopant, we smoothed away the singularity by using the potential $-e \cdot \tanh(\lambda r)/(4\pi\epsilon r)$ with a characteristic length scale $1/\lambda = 2.75\,\mathrm{nm}$, giving a well depth of 44 meV. These parameters are comparable to the Bohr radius $a_0^* = 1.9\,\mathrm{nm}$ and to shallow dopant ionisation energies. We randomly generate a set of dopant positions and calculate a bare dopant potential landscape ϕ_d in the absence of electrons. An example of two-dimensional potential landscape $\phi_\mathrm{d}(x, y)$ calculated at $z = 20\,\mathrm{nm}$ is shown in Fig. 1. The electron density $\rho(\boldsymbol{r})$ can then be evaluated for a range of Fermi energies by self-consistently solving the Thomas–Fermi approximation in two-dimension at $T = 0\,\mathrm{K}$:

$$\rho(\boldsymbol{r}) = \frac{m^* e^2}{\pi\hbar^2}[\mu - \phi_\mathrm{total}(\boldsymbol{r}, \rho)], \tag{2.1}$$

where $e \cdot \mu$ is the Fermi energy, $\phi_\mathrm{total}(\boldsymbol{r}, \rho)$ is the total electrostatic potential and is the sum of the potential due to the electrons and the local dopant potential. We used electron effective mass $m^* = 0.32828 m_\mathrm{e}$ and the dielectric constant $\epsilon_\mathrm{r} = 11.9$ for silicon, and solved the equation by a relaxation procedure on a grid of 1 nm pitch for a 20 nm × 400 nm section of two-dimensional electron gas (2DEG). Periodic boundary conditions were used at the ends of the 400 nm section which enable an infinitely long thin wire to be simulated.

We chose Fermi energies based on a fitted distribution of bare dopant potentials $\phi_\mathrm{d}^\mathrm{c}$ along the centre line of random wires. The mean $\overline{\phi_\mathrm{d}^\mathrm{c}}$ is linear in the number density of dopants N_d and the standard deviation $\sigma_\mathrm{d}^\mathrm{c}$ was fitted to $\sqrt{N_\mathrm{d}}$. We then chose ten Fermi energies equally spaced in the range $[e\overline{\phi_\mathrm{d}^\mathrm{c}} + e\sigma_\mathrm{d}^\mathrm{c}/2,\ e\overline{\phi_\mathrm{d}^\mathrm{c}} + 3e\sigma_\mathrm{d}^\mathrm{c}]$. We will present data on donor concentrations of 1, 3, 7 and $10 \times 10^{25}\,\mathrm{m}^{-3}$, for which the Fermi energy spacings are 2 meV, 37 meV, 56 meV and 67 meV. With finite V_ds, the island structure will be distorted but we have ignored this in our analysis as a self-consistent I–V solution would be required and would be computationally very expensive.

3. Structural Results for Periodic Structure

A typical sample result from the electron density calculation is shown in Fig. 2. Donor concentration N_d is assumed to be $10^{26}\,\mathrm{m}^{-3}$. In Fig. 2, we define a threshold electron density of $0.001\,\mathrm{Cm}^{-2}$ at the edge of an island. The near-continuous case seen in Fig. 2(a) breaks up into a linear chain of islands that merge and disappear as the wire becomes successively more depleted as shown in Figs. 2(b)–2(e). It should be noted that the electron distribution is described as a quasi-linear chain of a multiple electron islands. The reason why the electron distribution generally shows one-dimensional nature along the wire is simply explained as follows. In the limit of a jellium model for dopants, the bare dopant potential ϕ_d is given by $d^2\phi_\mathrm{d}/dx^2 \propto N_\mathrm{d}$, with N_d being the constant dopant concentration within the nanowire rectangular parallelepiped. Thus ϕ_d varies quadratically with x, resulting in parabolic-like confinement potential in cross-section. In the case of random dopants with a gate, it is no longer a true parabola as seen in Fig. 1, but is still similarly shaped. Another set of sample results are shown in Figs. 3(a)–3(e) for the nanowire with a lower donor concentration of $10^{25}\,\mathrm{m}^{-3}$. Generally, at lower dopant densities, the islands tend to be broader, but still mostly form linear chains. By comparing Fig. 3 with Fig. 4 it can be seen that the confinement potential is steeper and so the islands are narrower at a higher dopant density.

In Fig. 4, we show the mean of the number of islands formed in the nanowire using data from a set of 24 random dopant distributions. It is found that the number of islands decreases monotonically with increasing the Fermi energy (i.e., increasing the gate bias), and also decreases with an increase in donor concentration. We see that electron islands are still formed even for the highest Fermi energy corresponding to $3e\sigma_\mathrm{d}^\mathrm{c}$ above the mean of the bare dopant potential down the centre-line of the wire $e\overline{\phi_\mathrm{d}^\mathrm{c}}$. We studied the conditions on which the channel changes from continuous to discontinuous-island case. It was found that the number of continuous-island cases is zero for less than a specific Fermi energy and then rises in a monotonic fashion. In Fig. 4, for the lowest doping density of $10^{25}\,\mathrm{m}^{-3}$, the channel was discontinuous for all Fermi energies studied, whilst for the higher doping densities of 3, 7 and $10 \times 10^{25}\,\mathrm{cm}^{-3}$ the channels had their first continuous cases at about Fermi energy of $e\overline{\phi_\mathrm{d}^\mathrm{c}} + 2.5e\sigma_\mathrm{d}^\mathrm{c}$. For the

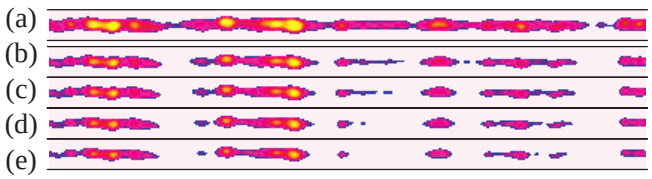

Fig. 2. An example solution: the electron density distribution is shown for Fermi levels $e\overline{\phi_\mathrm{d}^\mathrm{c}} + 3e\sigma_\mathrm{d}^\mathrm{c}$ (a) and four equally spaced levels in the closed range $[e\overline{\phi_\mathrm{d}^\mathrm{c}} + 4e\sigma_\mathrm{d}^\mathrm{c}/3,\ e\overline{\phi_\mathrm{d}^\mathrm{c}} + e\sigma_\mathrm{d}^\mathrm{c}/2]$ (b)–(e). All are plotted on the same density scale with a maximum of $0.04\,\mathrm{Cm}^{-2}$. The areas with electron density less than $0.001\,\mathrm{Cm}^{-2}$ are set to zero. The sample is 400 nm long and 20 nm wide with donor concentration of $10^{26}\,\mathrm{cm}^{-3}$.

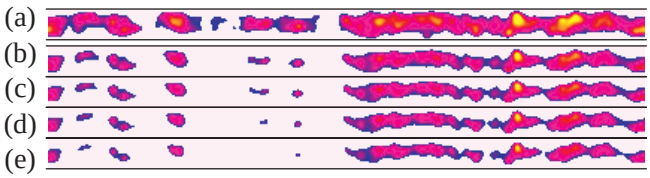

Fig. 3. Another example solution for the nanowire with donor concentration of $10^{25}\,\mathrm{m}^{-3}$: the electron density distribution is shown in the same manner as Fig. 2, except the maximum dencity scale is now $0.01\,\mathrm{Cm}^{-2}$.

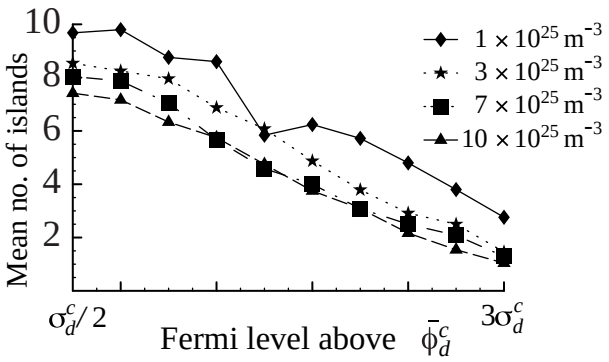

Fig. 4. The mean number of islands as a function of Fermi level for four different doping levels in a periodic structure of 400 nm long. The standard deviation for all Fermi levels and all dopant levels is about 2.

higher three doping densities and Fermi energy of $e\overline{\phi_{\rm d}^{\rm c}}+3e\sigma_{\rm d}^{\rm c}$, we only get 2, 4 and 4 continuous cases out of our 24 cases, respectively. The total area covered by the islands is found to be highly linear as a function of Fermi energy; however, the mean area of the individual islands is a monotonically increasing super-linear function.

4. Discussion on Threshold Voltage Distribution

To establish the threshold voltage $V_{\rm T}$ of the nanowire devices, it is necessary to make further assumptions. The first is that the islands are effectively metallic so that they do not distort when a finite source-drain bias is applied. We place electrodes with a size of 40 nm × 400 nm at the ends of the 20 nm × 400 nm nanowires and assume that this change in boundary conditions does not change the electron distribution. Next we calculate the capacitance matrix between all the islands and electrodes of this finite structure, and finally, very approximately, we take the tunnel resistance $R_{\rm T}$ as $R_{\rm T} = R_{\rm Q}\exp(d/\Lambda)$ where d is the chemical distance between islands and $\Lambda = 4\,{\rm nm}$ and $R_{\rm Q} = 25.4\,{\rm k}\Omega$. Chemical distance is the smallest number of steps taken in the x and y directions to get from one island to another without crossing another island. If $R_{\rm T} > 10^{16}\,\Omega$ then we set $R_{\rm T} \to \infty$. The tunnel resistance and capacitance matrices form the input to a Monte Carlo single electron transport simulator that includes only first order tunnelling processes. An iterative search method is used to find the source-drain bias $V_{\rm T}$ that first gives a 1 fA current at 4.2 K to a precision of $<200\,\mu$V. The simulation is repeated with a different set of random offset charges assigned to each island. The distribution of $V_{\rm T}$ can then be plotted for a particular combination of sample and Fermi energy. Ionised dopants in the depletion region induce offset charges on the islands. The dynamics of single electron systems are thought to restrict the offset charge to the range $|q_0| < e/2$ and as there are so many ionised dopants we would expect the induced offset charge to be distributed equally in this range.

In general, $V_{\rm T}$ decreases with increasing Fermi energy as the island sizes increase. However, anomalous results can occur when islands merge together and a single small island develops elsewhere with a much larger $V_{\rm T}$. The distribution of $V_{\rm T}$ for the structure shown in Fig. 2(e) is shown in Fig. 5(a). We note that the distribution has a peak around 50 mV, unlike a single island structure where the distribution would be flat. We are developing an analytical approach to $V_{\rm T}$ that predicts that the distribution is a piece-wise polynomial of maximum degree $N-1$, where N is the number of islands. For the case of Fig. 2(e) with $N = 7$ (the 'islands' at the ends of the diagram form part of the source and drain), the distribution of $V_{\rm T}$ can be approximated by a piece-wise linear function, for which $N = 2$. This suggests that the seven islands are grouped into two sets, i.e., the three on the left and the group of four on the right, with tunnel resistances between these 'macro' islands at least an order of magnitude larger than the tunnel resistances within the macro-islands as depicted in Fig. 5(b).

We have also examined to what extent the distribution obtained in Fig. 5(a) can be reproduced by using a two-island system by choosing capacitance parameters to match the energetics of the transitions. Figure 6 shows one of the sample

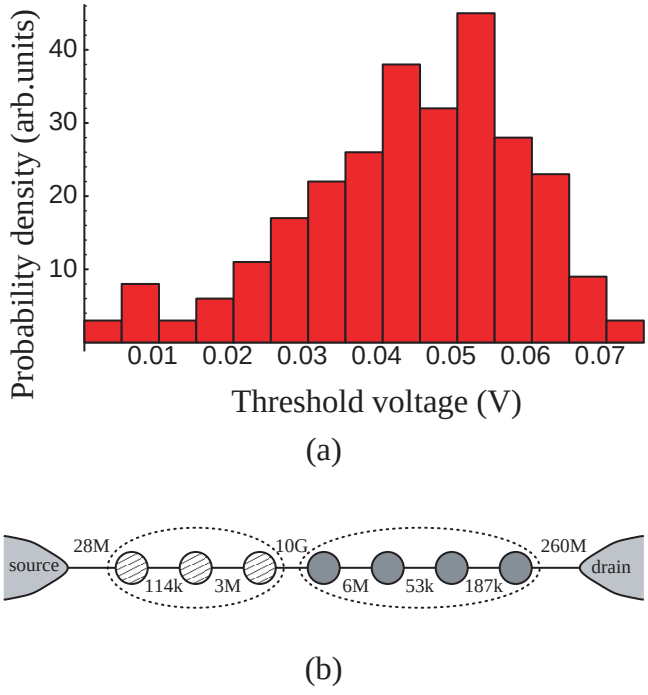

Fig. 5. (a) The distribution of threshold voltages as calculated for the (finite) structure in Fig. 2(e). 247 points have been used to form this histogram. (b) Schematic two-macro-island system with some of the smallest tunnel resistances (in Ω) between the seven islands. We have coloured the two 'macro-islands'.

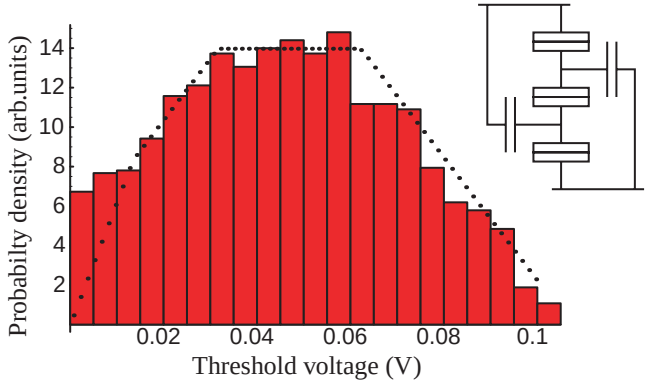

Fig. 6. The distribution of a two island system (inset) 'equivalent' to that shown in Fig. 4. The histogram is generated from a Monte Carlo simulation of the two-island system, the dotted curve represents the theoretical result.

results from a Monte Carlo simulation of the two-island system with the analytical results shown by a dotted line. The analytic method gives the maximum threshold voltage as,

$$V_{\rm T} = e\frac{C_{1\Sigma}+C_{2\Sigma}-C_{12}}{C_{1\Sigma}C_{2\Sigma}-C_{12}^2} - \frac{T_\Sigma}{e} \qquad (4.1)$$

where $C_{i\Sigma}$ is the sum of capacitances leading to node i, and C_{12} is the cross capacitance between the islands. T_Σ is a correction factor for finite definition of threshold current, and is given by $T_\Sigma = T_{s1} + T_{12} + T_{2d}$ where the indices s and d denote the source and drain electrodes and T_{ij} is the solution to,

$$\Gamma_{ij}(T_{ij}) = \frac{1}{e^2R_{ij}}\frac{-T_{ij}}{1-\exp(T_{ij}/k_{\rm B}T)} = I_{\rm th}/e \qquad (4.2)$$

where $I_{\rm th}$ is the threshold current of 1 fA, and Γ_{ij} is the first

order tunnelling transition rate formula from the global-view orthodox theory[1)] using R_{ij} as the tunnel resistance of the junction. This formula predicts a maximum threshold voltage of 98 meV, while the maximum threshold voltage from the Monte Carlo simulation was 104 meV, showing good agreement.

However, we could not obtain a good agreement with the results in Fig. 5(a) although the mean value of V_T for the seven-island system and the 'equivalent' two-island system are roughly the same. We consider that the details of the distribution in Fig. 5(a) cannot be described by using a simple two-island system despite the intuitive classification of the seven islands into two macro-islands. More detailed investigation of the V_T distribution remains as a future work.

5. Conclusion

A mechanism of natural formation of electron islands in the silicon nanowires has been demonstrated by using a numerical simulation in which random ionized dopants are treated explicitly. It has been shown that a virtually linear array of multiple electron islands are formed in the nanowires, and the one-dimensional geometrical nature stands out more for higher doping concentrations. The offset charge effects on the current threshold of the nanowire transistors have been investigated by combining these calculations of the electron islands with a Monte Carlo single electron circuit simulation. The obtained threshold voltage distribution has been discussed in terms of a macro-islands system consisting of several smaller islands connected one another.

Acknowledgements

The authors would like to thank Dr. J. R. A. Cleaver for the many helpful comments he made on the preparation of this manuscript.

1) *Single Charge Tunneling—Coulomb Blockade Phenomena in Nanostructures*, eds. H. Grabert and M. H. Devoret (Plenum, New York, 1991) NATO ASI Series B.
2) D. V. Averin and K. K. Likharev: J. Low Temp. Phys. **62** (1986) 345.
3) K. K. Likharev: IEEE Trans. Magn. **23** (1987) 1142.
4) M. R. Graham and H. Ahmed: Appl. Phys. Lett. **72** (1998) 3350.
5) H.-O. Müller, K. Katayama and H. Mizuta: J. Appl. Phys. **84** (1998) 5603.
6) H.-O. Müller, D. Williams and H. Mizuta: Jpn. J. Appl. Phys. **39** (2000) L723.
7) D. M. Pooley, H. Ahmed, H. Mizuta and K. Nakazato: Appl. Phys. Lett. **74** (1999) 2191.
8) R. Smith and H. Ahmed: J. Appl. Phys. **81** (1997) 2699.
9) N. J. Stone, H. Ahmed and K. Nakazato: IEEE Electron Device Lett. **20** (1999) 583.
10) Z. Durrani, A. Irvine, H. Ahmed and K. Nakazato: Appl. Phys. Lett. **74** (1999) 1293.
11) Z. Durrani, A. Irvine and H. Ahmed: IEEE Trans. Magn. **47** (2000) 2334.
12) K. Tsukagoshi, B. Alphenaar and K. Nakazato: Appl. Phys. Lett. **73** (1998) 2515.
13) J. A. Nixon and J. H. Davies: Phys. Rev. B **41** (1990) 7929.